Macromolecules

ARTICLE

pubs.acs.org/Macromolecules

One-Pot Synthesis of Poly(methacrylic acid-*co*-poly(ethylene oxide) methyl ether methacrylate)-*b*-polystyrene Amphiphilic Block Copolymers and Their Self-Assemblies in Water via RAFT-Mediated Radical Emulsion Polymerization. A Kinetic Study

Wenjing Zhang,[†] Franck D'Agosto,[†] Olivier Boyron,[†] Jutta Rieger,[‡] and Bernadette Charleux*,[†]

[†]C2P2 (Chemistry, Catalysis, Polymers & Processes), UMR 5265, Université de Lyon, Univ Lyon 1, CPE Lyon, CNRS, Team LCPP Bat 308F, 43 Bd du 11 novembre 1918, 69616 Villeurbanne, France

[‡]Laboratoire de Chimie des Polymères, UPMC Univ. Paris 6, UMR 7610, Sorbonne Universités and CNRS, 3 rue Galilée, 94200 Ivry, France

Supporting Information

ABSTRACT:

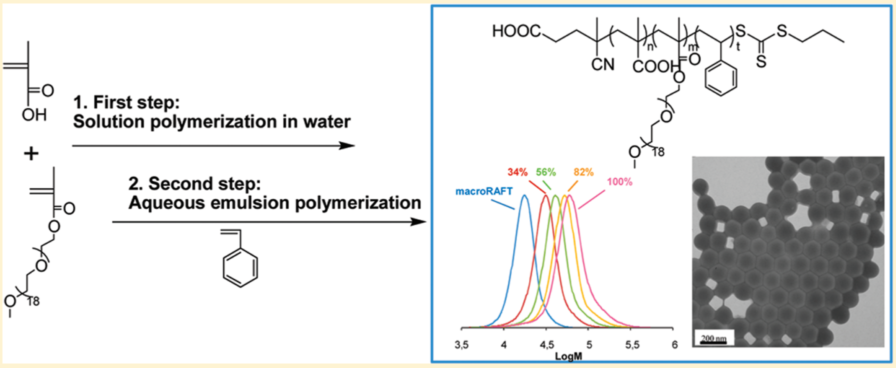

The RAFT-mediated emulsion polymerization of styrene was carried out in a one-pot, two-step procedure using two poly(methacrylic acid-*co*-poly(ethylene oxide) methyl ether methacrylate) macroRAFT agents of different compositions carrying a reactive trithiocarbonate end-group. The latter were prepared *in situ*, directly in aqueous solution at acid pH. In all cases, the synthesis was fast and efficient, leading to very high conversions and very good control over the polymer features. It was moreover particularly reproducible, which is an important outcome for the robustness of the method. Then, styrene was added and directly polymerized in the formed emulsion system until very high conversion in short reaction time. The method led to amphiphilic block copolymers, self-assembled into stable spherical particles. The diameter of the latter was directly governed by the initial concentration of macroRAFT agent, which also controlled the molar mass of the polystyrene block at constant styrene initial concentration. The emulsion polymerization step was studied in detail to provide information on the overall mechanism: nucleation, conversion rate, and chain growth. Because of the reduction of the number of synthesis and purification steps and of the overall reaction time, and due to the use of water as the sole reaction medium, the proposed method is of high interest in terms of both respect of environmental constraints and energy saving.

INTRODUCTION

The development of controlled/living free radical polymerization (CRP)[1−5] in aqueous emulsion systems has attracted much interest in the past 10 years due to the multiple advantages of the process (among others, it is environmentally friendly and favors high rates along with low viscosity) and the large number of industrial applications of the products.[6] Moreover, new possibilities are offered by the combination of both approaches.[7−14] For instance, the generation of amphiphilic block copolymers *in situ*, by taking advantage of the reactivity of water-soluble polymers tailored by CRP, leads to a new way of performing surfactant-free emulsion polymerization. The method leads to self-stabilized particles and can allow high solids content to be achieved, even under batch conditions. This strategy has been employed using the various CRP techniques available (mainly nitroxide-mediated radical polymerization,[15−20] organotellurium-mediated radical polymerization,[21,22] and RAFT for reversible addition−fragmentation chain transfer[23−36]). Most

Received: July 3, 2011
Revised: August 23, 2011
Published: September 07, 2011

Table 1. Experimental Conditions and Results for the Solution Copolymerizations of Methacrylic Acid (MAA) and Poly(ethylene oxide) Methyl Ether Methacrylate (PEOMA) in Water at 80 °C[a]

entry	MAA/PEOMA[b]	$[\text{MAA} + \text{PEOMA}]_0$ (mol L^{-1})	$[\text{MAA}]_0/[\text{CTPPA}]_0$	$[\text{PEOMA}]_0/[\text{CTPPA}]_0$	conv[c] (%)	$M_{n,th}$[d] (kg mol^{-1})	M_n^{LS}[e] (kg mol^{-1})	M_w/M_n[f]
A1-1	50/50	0.4	16	15	97	15.9	20.4	1.13
A2-1			16	15	96	15.7	20.6	1.08
A3-1			16	15	98	16.3	23.0	1.09
A4-1			15	15	97	15.7	20.5	1.09
A5-1			16	15	96	16.2	22.4	1.09
B1-1	67/33	0.6	28	14	97	15.6	23.1	1.13
B2-1			28	14	98	15.6	23.0	1.14
B3-1			29	14	98	15.8	23.8	1.12
B4-1			28	14	97	15.7	21.0	1.14
B5-1			29	14	98	15.8	22.4	1.10

[a] Polymerizations were run for 120 min. $[\text{ACPA}]_0$ = 2.66 mM for A1−A5 with MAA/PEOMA = 50/50 mol/mol and 2.84 mM for B1−B5 with MAA/PEOMA = 67/33 mol/mol. [b] MAA/PEOMA: molar ratio. [c] Overall molar monomer conversion determined by ^{1}H NMR. [d] Theoretical M_n calculated at 100% conversion of MAA and PEOMA. [e] M_n^{LS}: number-average molar mass determined by SEC in THF with RALS/LALS detectors, using dn/dc = 0.062 mL g^{-1} for A1−A5 with MAA/PEOMA (50/50 mol/mol) and dn/dc = 0.066 mL g^{-1} for B1−B5 with MAA/PEOMA (67/33 mol/mol), respectively. [f] M_w/M_n, determined by SEC in THF with a PS calibration.

of the time, it led to spherical particles analogous to crew-cut micelles. In addition, quite recently new morphologies could be achieved such as vesicles and very long nanofibers, which had never been obtained before via classical emulsion polymerization.[37−40]

In this article we will focus on the RAFT method, which has received an enormous interest from the polymer chemists community due to its versatility and the simplicity of the experimental conditions under which it can be carried out.[3] Actually, RAFT in emulsion polymerization has been successful only recently, thanks to the pioneer work of Hawkett and Gilbert et al.[23,24,26,27] It was generally necessary to adjust carefully the conditions and to have recourse to semicontinuous or seeded polymerization processes in order to reach both controlled polymerization features and particle stability. Among the experimental parameters, the pH value was shown to be important in case of use of acrylic acid-based macroRAFT agents, for both the colloidal stability and the polymerization control.[32,33] More recently, our works showed that styrene and *n*-butyl acrylate emulsion polymerizations could be fast and well-controlled in *ab initio* batch conditions using poly(ethylene oxide), PEO,[29,31] poly(*N*,*N*-dimethylacrylamide),[35] or poly(methacrylic acid-*co*-poly(ethylene oxide) methyl ether methacrylate), P(MAA-*co*-PEOMA),[39] macroRAFT agents prepared previously in solution polymerization.[41] In this manner, well-defined amphiphilic diblock copolymers could be achieved, forming self-stabilized polymer particles.

With the aim of simplifying and shortening this appealing process and making it even more environmentally friendly, we very recently proposed a new synthesis strategy, in which both polymer segments are synthesized in one pot in water, without the need for isolating and purifying the first block.[42,43] It was for instance demonstrated that the hydrophilic poly((meth)-acrylic acid) or P(MAA-*co*-PEOMA) macroRAFT agents and the derived amphiphilic diblock copolymers containing a hydrophobic polystyrene (PS) segment could be synthesized in a one-pot, two-step process directly in water, in very short reaction times, with high final conversions and high structural quality in both steps.

Our goal is now to study the kinetics and mechanism of the preparation of amphiphilic P(MAA-*co*-PEOMA)-*b*-PS block copolymers and their self-assemblies by the proposed one-pot process performed entirely in water. Special attention has been given to the emulsion polymerization step. Two types of macroRAFT agents have been used in this work, differing essentially in their composition. The purpose is to illustrate the advantages of the one-pot procedure and to better understand the nucleation and particle growth processes.

EXPERIMENTAL PART

Materials. Methacrylic acid (Acros, 99.5%), poly(ethylene oxide) methyl ether methacrylate (PEOMA, with 19 ethylene oxide units on average, M_n = 950 g mol^{-1}) (Aldrich), 4,4-azobis(4-cyanopentanoic acid) (ACPA, >98%, Fluka), sodium hydrogen carbonate (NaHCO_3, >99.7%, Aldrich), sodium 1-propanethiolate (Aldrich, 95%), carbon disulfide (Aldrich, 99%), and potassium hexaferricyanide (Aldrich, 99%) were used as received. Styrene (S, 99%, Aldrich) had the inhibitor removed by passing through an aluminum oxide column. Water was deionized before use (Purelab Classic UV, Elga LabWater). The RAFT agent 4-cyano-4-thiothiopropylsulfanylpentanoic acid (CTPPA) was obtained by reaction of ACPA with bis(propylsulfanylthiocarbonyl) disulfide synthesized in a first step, according to the literature.[41,44]

One-Pot, Two-Step Synthesis of P(MAA-*co*-PEOMA)-*b*-PS Amphiphilic Diblock Copolymers in Water (Series A and B). The experiments are labeled Ax-1 and Bx-1 (or Ax-2 and Bx-2), where A and B correspond to the composition of the macroRAFT agent (A for MAA/PEOMA = 50/50 mol/mol and B for MAA/PEOMA = 67/33 mol/mol), *x* corresponds to the experiment number, and 1 or 2 denotes the step number.

First Step: RAFT Solution Copolymerization of MAA and PEOMA in Water (Entries Ax-1 and Bx-1). A typical example (Table 1, entry B2-1) for the procedure is as follows: MAA (0.3535 g, 4.0 mmol), PEOMA (1.9054 g, 2.0 mmol), CTPPA (40.8 mg, 0.15 mmol), ACPA (8.2 mg, 0.029 mmol), and water (8.046 g) were added into a 50 mL round-bottom septum-sealed flask equipped with a magnetic bar. 1,3,5-Trioxane (111.5 mg, 1.2 mmol) was also added into the flask as an internal reference for determination of the monomer conversion by ^{1}H NMR. The solution was purged for 30 min with nitrogen and then heated to 80 °C in a thermostated oil bath under stirring (375 rpm). The final monomer conversions were determined by ^{1}H NMR and were close to 100% after 120 min reaction time.

Table 2. Aqueous Emulsion Polymerizations of Styrene (S) in the Presence of P(MAA-*co*-PEOMA) MacroRAFT Agents Formed in Water in the First Polymerization Step[a]

entry	[macroRAFT]$_0$[b] (mM$_{H_2O}$)	[S]$_0$/[macroRAFT]$_0$[b]	τ[c] (wt %)	t (min)	conv[d] (%)	$M_{n,th}$[e] (kg mol^{-1})	M_n^{LS}[f] (kg mol^{-1})	M_w/M_n[g]	d*n*/d*c* (mL g^{-1})	D_z[h] (nm)	σ[h]
					MAA/PEOMA = 50/50 mol/mol (Series A)						
A1-2	13.3	150	25.1	67	71	31.5	32.5	1.18	0.113	35	0.23
			27.5	75	87	34.1	34.7	1.17	0.119	37	0.24
			29.4	270	98	35.7	35.9	1.15	0.123	37	0.24
A2-2	6.24	330	19.1	70	75	46.8	46.1	1.23	0.137	74	0.08
			21.6	85	91	52.4	51.9	1.21	0.143	75	0.08
			22.5	180	97	54.4	54.8	1.19	0.144	76	0.07
A3-2	3.33	590	14.5	70	62	61.1	86.0	1.21	0.149	105	0.05
			17.5	90	80	72.1	103.0	1.23	0.155	108	0.06
			18.2	210	90	78.5	106.8	1.20	0.158	110	0.07
A4-2	2.46	790	11.9	90	53	64.4	68.8	1.14	0.153	144	0.04
			16.3	120	80	86.2	94.2	1.14	0.162	151	0.02
			19.2	200	97	100.4	107.1	1.16	0.165	156	0.03
A5-2	2.00	970	11.9	120	55	78.1	78.1	1.13	0.158	152	0.04
			14.8	150	72	95.3	100.2	1.20	0.163	160	0.02
			17.8	300	90	113.4	117.2	1.18	0.168	166	0.02
					MAA/PEOMA = 67/33 mol/mol (Series B)						
B1-2	13.3	150	25.6	66	76	34.9	30.1	1.18	0.118	64	0.24
			28.4	90	95	37.8	38.2	1.20	0.125	66	0.21
			28.9	300	98	38.3	39.7	1.24	0.125	67	0.21
B2-2	6.67	300	17.6	68	61	42.0	40.8	1.23	0.132	128	0.04
			20.0	78	76	46.7	45.9	1.27	0.138	128	0.03
			22.8	210	94	52.4	58.9	1.35	0.144	131	0.05
B3-2	5.00	400	15.9	70	60	48.6	47.8	1.24	0.139	126	0.07
			19.0	85	79	56.5	58.0	1.26	0.147	133	0.04
			21.4	180	94	62.4	68.8	1.32	0.151	130	0.03
B4-2	4.00	500	14.1	70	56	52.2	50.9	1.37	0.144	123	0.05
			18.4	90	82	66.0	66.9	1.26	0.154	132	0.01
			21.4	230	100	75.3	77.4	1.31	0.158	135	0.01
B5-2	3.33	600	13.5	95	56	57.2	58.8	1.26	0.149	156	0.02
			18.4	150	85	75.6	79.8	1.30	0.158	168	0.009
			20.0	210	95	81.5	83.9	1.32	0.161	174	0.005

[a] See Table 1 for details. The polymerizations were performed at various [S]$_0$/[macroRAFT]$_0$ ratios at 80 °C, with [styrene]$_0$ = 2 M$_{H_2O}$; ACPA added in the second step: [macroRAFT]$_0$/[ACPA]$_{0,\text{2nd step}}$ = 5; overall ACPA amount: [macroRAFT]$_0$/[ACPA]$_{0,\text{total}}$ = 2.5; pH = 3.5. [b] The concentration of the macroRAFT agent in the emulsion polymerization step was calculated on the basis of the initial amount of the CTPPA RAFT agent in the first step. [c] Experimental solids content in wt % based on the overall weight of latex: [*m*(polystyrene) + *m*(macroRAFT)]/*m*(latex). [d] Monomer conversion determined by gravimetry. [e] Theoretical number-average molar mass, $M_{n,th}$, calculated using the experimental conversion. [f] M_n^{LS} determined by SEC in THF with RALS/LALS detectors. [g] M_w/M_n determined by SEC in THF with a PS calibration. [h] D_z is the Z-average particle diameter, and σ is the dispersity factor derived from dynamic light scattering.

Second Step: RAFT Emulsion Polymerization of Styrene in Water (Entries Ax-2 and Bx-2). All experiments are summarized in Table 2, while the present description corresponds to the typical experiment B2-2. Styrene (4.6031 g, 44 mmol), ACPA (8.2 mg, 0.029 mmol), $NaHCO_3$ (8.6 mg, 0.10 mmol), and 13.9 g of water were added into a round-bottom septum-sealed flask and purged for 30 min with nitrogen in an ice bath. Then, after 120 min of reaction in the first step (B2-1), the so-prepared mixture was injected under nitrogen into the reaction flask. For the other experiments, the amounts of styrene, ACPA, $NaHCO_3$ and water were adapted to target the final concentrations reported in Table 2. The polymerization was performed at 80 °C and finally quenched after 3.5 h by immersion of the flask in iced water. The conversion of styrene was determined by gravimetric analysis. After drying and subsequent methylation of the COOH groups,[45] the polymers were analyzed by size exclusion chromatography in THF solution, and M_n^{LS} was derived from combined light scattering (LS) and refractive index (RI) signals, while M_w/M_n was calculated with a calibration curve based on polystyrene standards. The refractive index increment (d*n*/d*c* = ν) for well-defined block copolymers was calculated according to $dn/dc = w_x\nu_x + w_y\nu_y$, where w is the weight fraction of P(MAA-*co*-PEOMA) (x with ν_x = 0.062 mL g^{-1} for macroRAFT agent A1-1 to A5-1 (with MAA/PEOMA = 50/50 mol/mol) and ν_x = 0.066 mL g^{-1} for macroRAFT agent B1-1 to B5-1 (with MAA/PEOMA = 67/33 mol/mol) and polystyrene (y with ν_y = 0.185 mL g^{-1}).

Scheme 1. Schematic Representation of the One-Pot Synthesis of Poly(methacrylic acid-*co*-poly(ethylene oxide) methyl ether methacrylate)-*b*-polystyrene, P(MAA-*co*-PEOMA)-*b*-PS, Copolymers via Successive Aqueous Solution and Emulsion Polymerizations

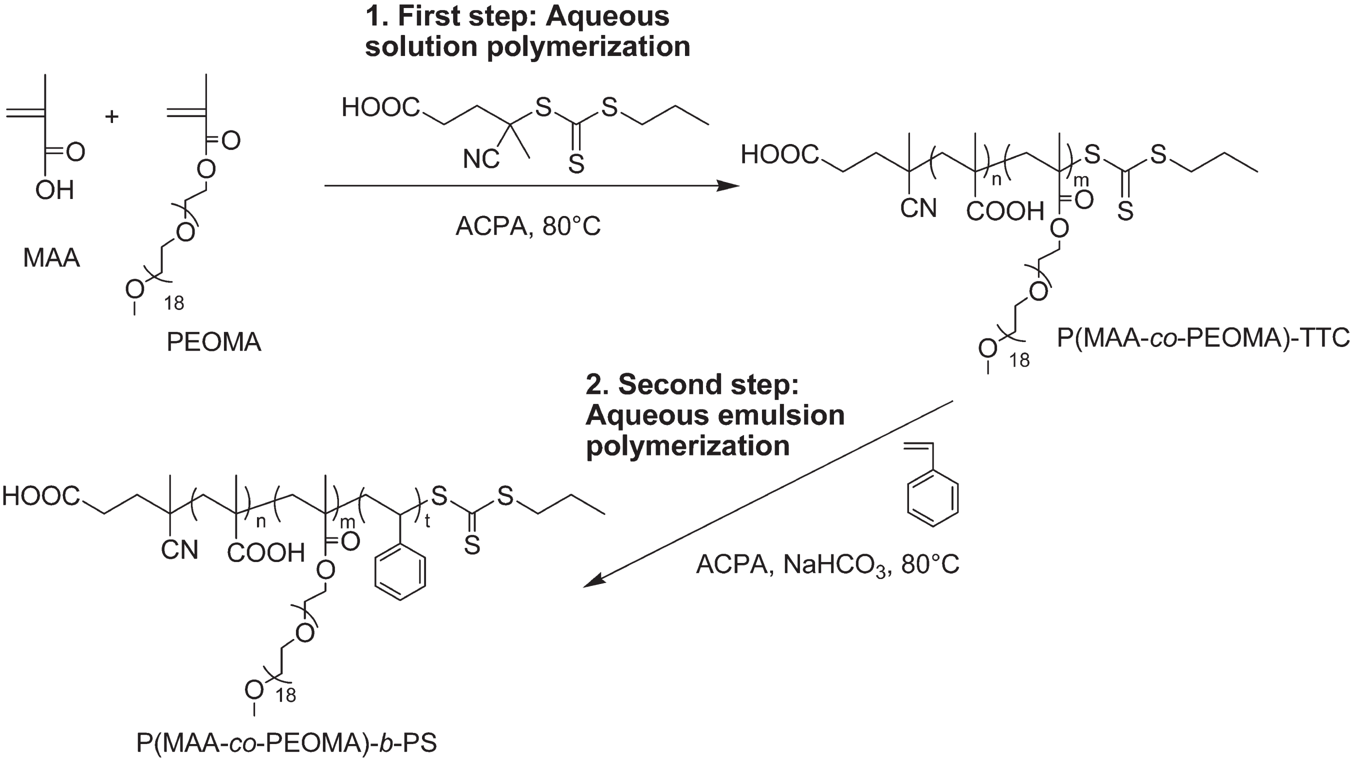

Characterization Techniques. The overall monomers MAA and PEOMA conversion at $t = 2$ h was determined by ^{1}H NMR spectroscopy of the crude reaction medium in D_2O at room temperature (Bruker DRX 300) in 5 mm diameter tubes. The chemical shift scale was calibrated relative to tetramethylsilane, and the vinyl protons of the monomers were used to determine the overall conversion, using 1,3,5-trioxane as an internal reference.

Size exclusion chromatography (SEC) measurements were performed with a Viscotek TDAmax system from Malvern Instruments that consists of an integrated solvent and sample delivery module (GPCmax) and a Tetra Detector Array (TDA) including a right angle (90°) and a low angle (7°) light scattering detector (RALS/LALS), a 4-capillary differential viscometer, a differential refractive index detector (RI), and a diode array UV detector. THF was used as the mobile phase at a flow rate of 1 mL min^{-1}, and toluene served as a flow rate marker. All polymers were injected at a concentration of 3 mg mL^{-1} after filtration through a 0.45 μm pore-size membrane. The separation was carried out on three Polymer Laboratories columns [3 × PLgel 5 μm Mixed C (300 × 7.5 mm)] and a guard column (PL gel 5 μm). Columns and detectors were maintained at 40 °C. The OmniSEC 4.6 software was used for data acquisition and data analysis. The polydispersity indexes, M_w/M_n, were calculated with a calibration curve based on narrow polystyrene (PS) standards (from Polymer Laboratories), using only the refractometer detector. The absolute number-average molar masses, M_n^{LS}, were calculated using the RALS/LALS and RI signals. For the macroRAFT agents, the corresponding average refractive index increments (dn/dc) were measured with the online refractometer injecting polymer solutions (at a concentration $c = 3$ mg mL^{-1}) at four different injection volumes (50, 80, 100, and 120 μL). Then, dn/dc can be calculated, directly in the OmniSEC software, by plotting the RI area (integrated from the RI signal) versus the total amount of polymer injected. Because RI area is assumed to be proportional to the refractive index of the sample, the slope of this curve gives dn/dc. The reported M_n^{LS} correspond to the calculated non-methylated values. In the plot showing the evolution of M_n^{LS} with styrene conversion in the emulsion polymerization step, the straight line corresponds to the expected evolution of the theoretical number-average molar mass, $M_{n,th}$, calculated by the introduced mass of styrene multiplied by conversion divided by the initial mole number of RAFT agent (considered equal to the initial molar number of CTPPA) plus the molar mass M_n^{LS} of the macroRAFT agent.

For transmission electron microscopy (TEM) samples were dropped on a carbon-coated copper grid and dried under air. The TEM images were examined at an accelerating voltage of 80 kV with a Philips CM120 transmission electron microscope (Centre Technologique des Microstructures (CTμ), University Claude Bernard Lyon 1, Villeurbanne, France).

The particle size (average hydrodynamic diameter, D_z) and the dispersity of the sample (σ) were measured by dynamic light scattering (DLS, Nano-ZS from Malvern Instruments). The data were collected using the fully automatic mode of the Nano-ZS system. The autocorrelation functions were analyzed with the cumulant method. All samples were diluted with fresh deionized water, and all measurements were recorded at 285 K.

■ RESULTS AND DISCUSSION

This work aims at developing a simple and straightforward synthesis strategy, which allows the preparation of amphiphilic P(MAA-*co*-PEOMA)-*b*-PS block copolymer particles via a one-pot, surfactant-free, emulsion polymerization process using the RAFT technique. In a first step, a hydrophilic P(MAA-*co*-PEOMA)

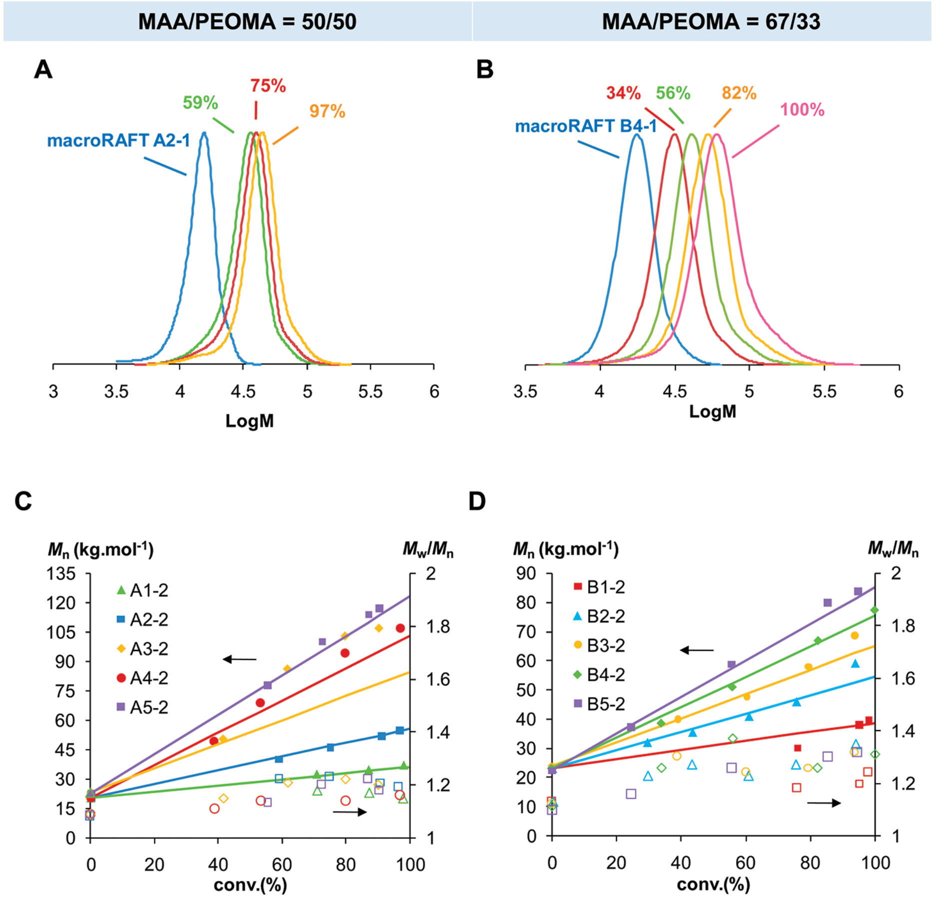

Figure 1. Synthesis of P(MAA-*co*-PEOMA)-*b*-PS diblock copolymers via aqueous RAFT emulsion polymerization of styrene using P(MAA-*co*-PEOMA) macroRAFT agents (MAA/PEOMA = 50/50 (left) and 67/33 (right)) formed in a first polymerization step in water. (A, B) Evolution of the size exclusion chromatograms with monomer conversion ($w(\log M)$ vs $\log M$) for sample A2-2 and B4-2. (C, D) Evolution of the number-average molar masses (M_n^{LS}) and polydispersity indexes (M_w/M_n) with monomer conversion in the second step. The straight lines correspond to the theoretical evolution of M_n vs conversion.

macromolecular RAFT agent (macroRAFT) is synthesized via an aqueous solution copolymerization of methacrylic acid (MAA) and poly(ethylene oxide) methyl ether methacrylate (PEOMA) until high conversion. Without purification, the synthesis of the second polymer block is performed in the same reactor via RAFT emulsion polymerization of styrene (Scheme 1). Two series of experiments with macroRAFT agents of different compositions (series A: MAA/PEOMA = 50/50 mol/mol; series B: MAA/PEOMA = 67/33 mol/mol) were performed in order to demonstrate the versatility of the proposed system and to investigate the main features of the kinetics of this RAFT emulsion polymerization performed in the complete absence of low molar mass surfactant.

First Step: RAFT Solution Copolymerization of MAA and PEOMA in Water. In the first polymerization step, P(MAA-*co*-PEOMA) macroRAFT agents were synthesized in aqueous solution in the presence of CTPPA, a trithiocarbonate RAFT agent, and ACPA as an initiator (see Table 1 for the experimental conditions). In an earlier study performed in the presence of hydrophobic RAFT agents with a reactive dithiobenzoate group (and a hydrophobic initiator),[46] we reported that the synthesis of such copolymers was better controlled in water compared to organic solutions. This was attributed to the formation of hydrophobic domains in which the polymerization occurred as in bulk. Here, the polymerizations were performed at 80 °C in conditions in which all components were fully water-soluble. In a preliminary investigation, the copolymerization kinetics were monitored by ^{1}H NMR spectroscopy (Supporting Information, Table SI-1 and Figure SI-1), and it appeared also that the polymerization was very fast and that complete conversions were reached within 2 h. Consistent with our earlier results,[46] no significant difference in reactivity of both monomers was detected. Copolymers composed of either equal amounts of MAA and PEOMA or 67 mol % MAA and 33 mol % PEOMA were prepared (Supporting Information Table SI-1) in which both comonomers should thus be statistically distributed in the polymer chains.

In the one-pot emulsion polymerization conditions, the polymerization kinetics were not followed in the first step. Nevertheless, before addition and polymerization of the hydrophobic monomer in the same reactor (i.e., after 120 min of reaction time), a sample was withdrawn in order to determine (i) the hydrophilic monomers molar conversion by ^{1}H NMR and (ii) the macromolecular characteristics of the formed macroRAFT agent by SEC using a light scattering detector (number-average molar mass, M_n^{LS}, and polydispersity index, M_w/M_n). For both series of copolymers (A and B), the experimental M_n^{LS} values were similar and ranged between 20 and 24 kg mol^{-1} as determined by SEC, with very low polydispersity indexes (Table 1). In

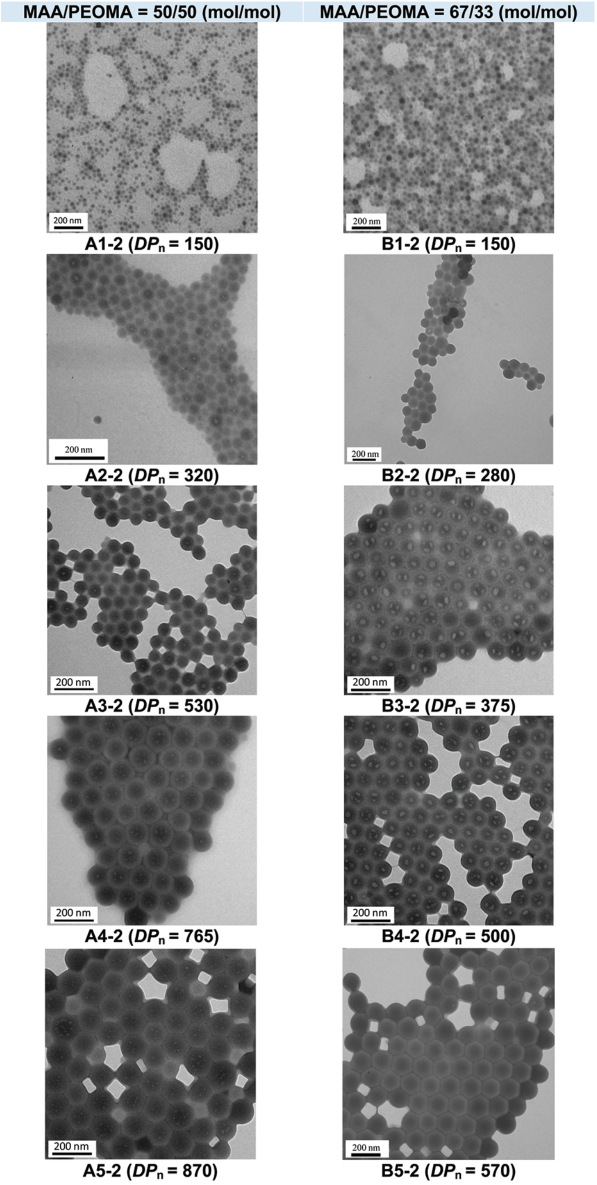

Figure 2. TEM images of the final P(MAA-*co*-PEOMA)-*b*-PS particles obtained by one-pot two-step polymerization via RAFT in water (the reported DP_n are the calculated ones based on the final conversion from gravimetric analysis).

Table 1, it can be noticed that, for both macroRAFT agent compositions, the results were very reproducible, showing the robustness of the synthesis, which is an important outcome for such a one-pot process.

Second Step: RAFT Emulsion Polymerization of Styrene in Water. *Characteristics of the Formed Copolymers.* In the second polymerization step, different amounts of a styrene/water mixture (together with a second load of initiator) were introduced into the reactor in such a way that the resulting styrene concentration (apparent concentration expressed with respect to the water phase in $\mathrm{mol\ L^{-1}}_{\mathrm{H_2O}}$) was always 2 $\mathrm{mol\ L^{-1}}_{\mathrm{H_2O}}$. This led to different concentrations of the macroRAFT agents, i.e., different target degrees of polymerization for the hydrophobic polystyrene block, between 16 and 100 kg mol^{-1} (Table 2).

The final conversions of styrene were always very high in rather short reaction times (Table 2), indicating efficient polymerization. As shown by size exclusion chromatography (Figure 1A,B), the polymerizations exhibited the features of a living system with fast and quantitative reinitiation by the hydrophilic P(MAA-*co*-PEOMA) first block (no residual macroRAFT agent was detected for conversions higher than 30−40%) toward the formation of block copolymers, with an average molar mass that could be as high as 10^5 g mol^{-1}. In a similar way for both series and independently of the target molar mass of the polystyrene block, the experimental M_n^{LS} values increased linearly with monomer conversions and matched very well the theoretical values (see Figure 1C,D and Table 2). The polydispersity indexes remained very low, about 1.2 for series A and slightly higher (1.2−1.4) for series B. The proposed one-pot process performed exclusively in water is thus particularly efficient as it allows high conversions to be achieved in both steps together with high reinitiation efficiency, hence affording well-controlled amphiphilic P(MAA-*co*-PEOMA)-*b*-PS block copolymers, without unreacted water-soluble species.

Characteristics of the Polymer Dispersions. During the emulsion polymerizations of styrene and the formation of the hydrophobic blocks by chain extension, the polymerization systems became turbid with the progress of the reaction (except for sample A1-2, which was translucent), resulting eventually in very stable latexes. Although the reactions were performed in acidic conditions where the MAA subunits in the hydrophilic blocks are nonionized and most likely linked to ethylene oxide units (present in excess in both systems) via hydrogen bonding,[47,48] a good stabilization was imparted by the PEO segments present along the chains. It is known that self-assembly of amphiphilic block copolymers into micelles occurs rapidly for very low degrees of polymerization of the PS block.[49,50] The so-formed styrene swollen micelles constituted then the loci of the ongoing emulsion polymerization, and finally self-stabilized particles composed of P(MAA-*co*-PEOMA)-*b*-PS copolymers were obtained.

In all experiments, spherical particles with narrow particle size distribution (i.e., low polydispersity factors, σ) were observed as shown by the DLS (Table 2) and TEM analyses (Figure 2). Generally, the higher the initial styrene/macroRAFT agent molar ratio, i.e., the larger the DP_n (number-average degree of polymerization) of the polystyrene block, the narrower was the particle size distribution (lower values of σ; see Table 2). Furthermore, for both series, the final particle size increased significantly with the molar mass of the PS block (Table 2). For instance, for series A, very small particles of about 37 nm in diameter formed with short PS chains (target $DP_n = 150$), whereas particles in the range of 170 nm in diameter were obtained with target $DP_n = 970$ for the PS block (Table 2). This correlation between chain length (i.e., macroRAFT agent concentration) and particle size has already been observed earlier for very large particles composed of PEO-*b*-poly(*n*-butyl acrylate) copolymers (diameters in the 100−500 nm range)[29] but could not be clearly observed in other systems where small particles with diameter close to 100 nm were obtained.[34] Generally, the particle diameters measured by DLS were smaller for series A compared to those found for similar experiments of series B (compare A1-2 with B1-2, A2-2 with B2-2, and A3-2 with B5-2, Table 2 and Figure 2), indicating a larger number of formed particles, i.e., a larger stabilized surface area. As discussed above, the stability was mainly due to the presence of the PEO side chains in the hydrophilic copolymer stabilizer. In series B (when compared with series A), a PEO macromonomer

Table 3. Kinetic Values for the Aqueous RAFT Emulsion Polymerization of Styrene in the Presence of P(MAA-*co*-PEOMA) MacroRAFT Agents Formed *in Situ* in the First Polymerization Step

entry	$[\text{macroRAFT}]_0$ (mM_{H_2O})	DP_n[a]	$D_{n,\text{TEM}}$[b] (nm)	slope[c] ($10^{-4}\ s^{-1}$)	τ[d] ($g\ L^{-1}{}_{H_2O}$)	N_p[e] ($10^{17}\ L_{H_2O}{}^{-1}$)	$\tilde{n}$[f]	$A_{\text{macroRAFT}}$[g] (nm^2)	$N_{\text{macroRAFT}}$/particle[h]
A1-2	13.3	150	26	9.9	401	410	0.01	11	190
A2-2	6.24	320	45	6.5	293	58	0.04	10	600
A3-2	3.33	530	78	3.7	243	9.3	0.13	9	2200
A4-2	2.46	765	122	1.8	238	2.4	0.25	7	6300
A5-2	2.00	870	133	1.3	222	1.7	0.25	8	7300
B1-2	13.3	150	31	7.6	393	240	0.01	9	330
B2-2	6.67	280	94	4.0	300	6.6	0.20	5	6100
B3-2	5.00	375	93	4.1	276	6.2	0.22	6	4900
B4-2	4.00	500	96	3.5	272	5.6	0.21	7	4300
B5-2	3.33	570	143	1.5	252	1.9	0.26	5	10600

[a] Experimental DP_n of the polystyrene block. [b] Number-average particle diameter D_n measured by transmission electron microscopy (TEM); it is assumed to give a good estimation of the hydrophobic core diameter. [c] The slope (s^{-1}) is given by dconv/d*t* determined in the linear region of the monomer conversion vs time plot. [d] Experimental solids content, i.e., mass of polymer per L of water: $\tau = (m_{\text{macroRAFT}} + \text{conv }\% \times m_{\text{styrene}})/v_{\text{water}}$. [e] Number of particles per L of water: $N_p = (6 \times \tau)/(\pi \times D_{n,\text{TEM}}{}^3 \times d_p)$, with D_n the particle diameter measured from TEM, τ the mass of polymer per L of water, and d_p the PS density: $d_p = 1.05\ g\ cm^{-3}$ at 25 °C). [f] Average number of radicals per particle, $\tilde{n} = (\text{slope} \times N_A \times [M]_0)/(k_p \times N_p \times [M]_p)$, with N_A Avogadro's number, $[M]_0$ the initial molar concentration of monomer per L of water, $[M]_p$ the concentration of monomer in a particle, $[M]_p = 5.5\ \text{mol}\ L_p{}^{-1}$ at 50 °C for styrene,[6] k_p the propagation rate constant of styrene, $k_p = Ae^{-E_A/RT} = 662\ L_p\ \text{mol}^{-1}\ s^{-1}$ at 80 °C, $A = 4.27 \times 10^7$, $E_A = 32\,500\ J\ \text{mol}^{-1}$).[54] [g] Calculated average area (nm^2) per macroRAFT agent chain at the core particle surface. $A_{\text{macroRAFT}} = (\pi \times D_{n,\text{TEM}}{}^2)/N_{\text{macroRAFT}}$. [h] Calculated average number of macroRAFT agent chains per particle. $N_{\text{macroRAFT}} = ([\text{macroRAFT}]_0 \times N_a)/N_p$.

was replaced on average by 12–13 MAA units (see Table 1), which seems sufficient to change the behavior of the stabilizing block by making it more hydrophobic at pH 3.5. This offers a simple tool for easy and efficient control over particle size and number.

The average particle diameters were also determined by TEM analysis (see Figure 2 and the results reported in Table 3 for the final latexes). In contrast to DLS, TEM allows essentially the hydrophobic electron-dense PS core to be observed (therefore, the TEM diameters were smaller than those determined by DLS). As reported in Table 3, smaller core diameters were generally observed for series A compared to series B, for a similar PS molar mass. It can thus again be concluded that the composition of the macroRAFT agent has an impact on the particle formation and stabilization.

The fact that only spherical particles were observed (Figure 2) comes in contrast to the results obtained with the same type of macroRAFT agent (same structure with either 8 or 19 ethylene oxide units in the PEO side chains) used in the emulsion polymerization of styrene and published in a previous article, in which the formation of fibers and vesicles was reported.[39] While the other experimental conditions were comparable, the main differences were (i) the pH of the emulsion polymerization step (3.5 in this work as compared with 5 in the previous one) and (ii) the process (one-pot here versus the use of isolated and purified macroRAFT agents before). In our previous work, one experiment was performed at pH 3 using the macroRAFT agent with the shortest PEO segments (8 EO units) and showed essentially spheres with a very poor control of the polymer characteristics. In the present work, increasing the size of the PEO side chains strongly improved the quality of the polymerization, most probably by increasing the stabilizing efficiency of the hydrophilic chains at this low pH. Since the change in process cannot explain the change in morphology as demonstrated in the Supporting Information (the similar two-pot, two-step experiments also led to spherical particles), therefore pH (and hence conformation of the hydrophilic block) seems to be the most relevant parameter in this system to explain the obtained particle morphology.

Kinetics of the Emulsion Polymerizations. The kinetic features of the emulsion polymerizations of styrene were further examined and will be discussed in comparison with what is known for traditional emulsion polymerizations,[6] as our system strongly differs in terms of nucleation and type of polymer produced. The information might thus provide clues for the interpretation of the observed results. Conversion versus time plots in Figure 3A,B show that the kinetics were similar for both series. The graphs exhibited first a marked induction period of ~50 min, typical of the RAFT emulsion polymerizations performed in the presence of a water-soluble macroRAFT agent. This can be ascribed to the delayed nucleation, which starts only when the hydrophobic segment of the *in situ* created amphiphilic copolymers reach the critical size for self-assembly. Before that stage, the polymerization takes place essentially in the aqueous solution where the concentration of styrene is very low and hence propagation is not favored over chain transfer. When the polymerization started, it was generally very fast (overall duration of less than 3 h), and the higher the macroRAFT agent concentration, the faster the polymerizations. This feature was even more pronounced for series A than for series B. At this stage, the shape of the conversion versus time plots became essentially linear (corresponding to the interval II of an emulsion polymerization), and the slopes in the linear region were derived for all graphs and are reported in Table 3. All other values (number of particles, N_p, per latex unit volume and average number of radicals per particle, $\tilde{n}$) that are relevant to describe the polymerization kinetics are also reported in Table 3, which will thus allow discussion on a quantitative basis.

It is clear, from the kinetic results, that the polymerization rate (represented by the slope in the linear part of the conversion

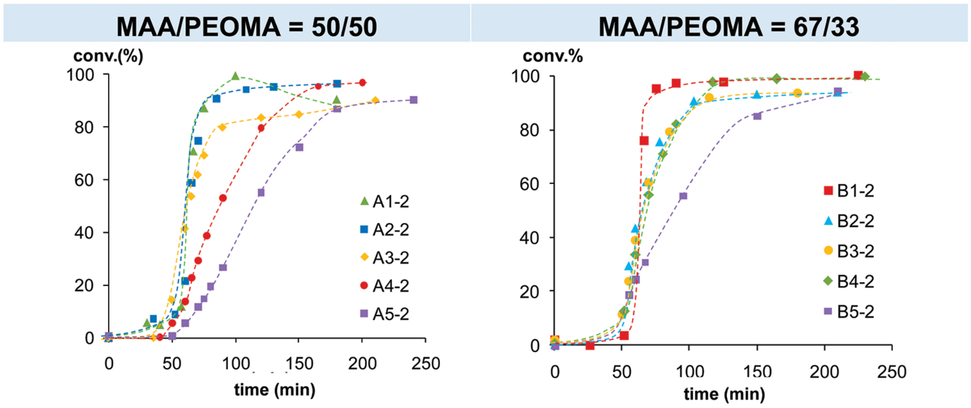

Figure 3. Evolution of styrene conversion with time for the synthesis of P(MAA-*co*-PEOMA)-*b*-PS diblock copolymers via aqueous RAFT emulsion polymerization of styrene in the presence of P(MAA-*co*-PEOMA) macroRAFT agents (MAA/PEOMA = 50/50 (left) and 67/33 (right)) formed in the first polymerization step in water (see Table 2).

versus time plots) was strongly affected by the number of particles per unit volume of latex (N_p in Table 3) and increased when the latter increased. N_p was directly influenced by the macroRAFT agent concentration (it increased when the latter was increased) and may have also been affected by the initiator concentration since the macroRAFT agent over initiator molar ratio was kept constant. The results allowed the average number of radicals per particle to be calculated (see $\tilde{n}$ in Table 3). The values, which were in the 0.01−0.26 range, increased when the particle size increased and were not substantially different for both series A and B. These results are quite normal in emulsion polymerization, for which the existence of more than 1 radical in a given particle on average results in instantaneous termination when the particle diameter is small.[6] The $\tilde{n}$ values were however lower than the expected 0.5 value,[6] which might be explained by an effect of the RAFT mechanism as already discussed previously by Luo et al.[51] although the use of trithiocarbonate RAFT agents may not induce rate retardation like dithiobenzoates actually do.

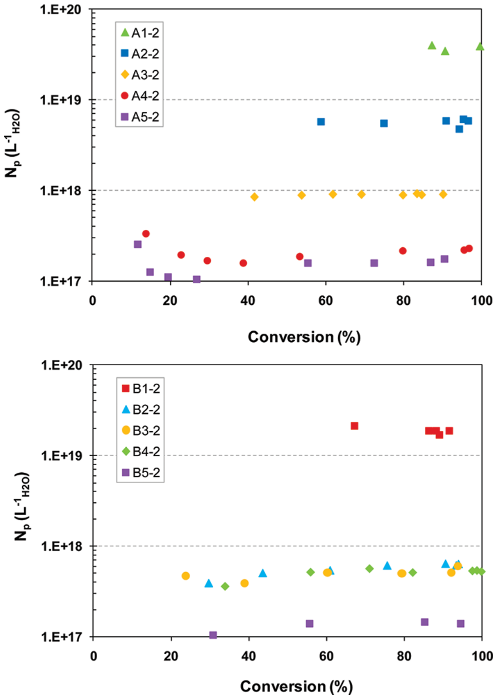

Figure 4. Evolution of the number of particles N_p per L of water phase versus monomer conversion for the synthesis of P(MAA-*co*-PEOMA)-*b*-PS diblock copolymers via aqueous RAFT emulsion polymerization of styrene in the presence of P(MAA-*co*-PEOMA) macroRAFT agents (top: series A with MAA/PEOMA = 50/50 mol/mol; bottom: series B with MAA/PEOMA = 67/33 mol/mol) formed *in situ* in the first polymerization step.

Most interesting are the calculated average number of macroRAFT agent chains ($N_{\text{macroRAFT}}$) (i.e., amphiphilic block copolymers) per particle and average area per hydrophilic segment ($A_{\text{macroRAFT}}$) at the particle core surfaces (Table 3). (Both calculations assume that all macroRAFT agent chains are consumed and located at the particle/water interfaces.) It appears that $N_{\text{macroRAFT}}$ significantly increased when the initial macroRAFT agent concentration was decreased and that in contrast $A_{\text{macroRAFT}}$ remained approximately constant (or slightly decreased) for a given series of experiments. $A_{\text{macroRAFT}}$ was however larger for series A (in which the macroRAFT agent contained more ethylene oxide units, i.e., with a more pronounced hydrophilic character at pH 3.5) than for series B. These results indicate that particle stabilization was essentially governed by surface coverage. If one assumes that particle nucleation starts by self-assembly of the *in situ* formed amphiphilic block copolymers, it is thus expected that micelles with similar aggregation numbers are initially formed in all emulsion polymerizations of a given series, due to structural and kinetic reasons. A simple calculation can indeed illustrate this assertion. In the very first stage of the polymerization, in the aqueous solution, the average number of styrene units added per active macroradical can be calculated by $\lambda = [\text{S}]_{\text{H}_2\text{O}}/(C_{\text{tr}}[\text{macroRAFT}]_{\text{H}_2\text{O}})$, in which C_{tr} in the chain transfer constant of the macroRAFT agent. $[\text{S}]_{\text{H}_2\text{O}}$ being below 10 mM at saturation and taking $C_{\text{tr}} = 10$ as a minimum value,[52] it comes that λ is below 1 in all experiments. Considering that the macroRAFT agent presents a higher chain transfer constant than the created polystyrene−trithiocarbonate end-group in the radical polymerization of styrene, a very high crossover efficiency is expected, along with a slow growth of the PS blocks. Thus, (i) nucleation by self-assembly is favored over formation of nuclei by precipitation of a few chains having reached the critical degree of polymerization (i.e., homogeneous nucleation; see ref 22 for analogous discussion in the case of organotellurium-mediated radical emulsion polymerization) and (ii) all emulsion polymerizations of the same series will form amphiphilic block copolymers with similar structure, leading to aggregates expected to be also similar. Then, after nucleation and upon polystyrene chain growth and hence expansion of particle volume and surface, an increased number of hydrophilic chains becomes necessary for a given particle to maintain colloidal stability. Two mechanisms may then take place to meet this condition: (i) adsorption at the surface of already created particles of individual chains reaching the critical size or (ii) coagulation and coalescence of formed particles (made possible by the presence of monomer that swells and hence plasticizes the core). This second possibility can be supported by the fact that the final number of particles as a function of monomer conversion remained constant at high conversion (Figure 4) but exhibited a decrease (note the logarithmic scale in Figure 4) at low conversion, typically below 20% when those conversions could be measured (experiments A4-2 and A5-2 with a low polymerization rate). In the same vein, the low polydispersity indexes of the copolymers along with the complete shift of the SEC peaks from the macroRAFT agent toward the growing amphiphilic block copolymers gives a good support to the second possibility. If the phenomenon takes place during the first 20% conversion, it still remains difficult to conclude definitively and the first possibility can however not be ruled out. In other words, nucleation and particle growth appear to be governed by self-assembly of amphiphilic block copolymer chains with short hydrophobic block, followed by adsorption of amphiphilic copolymer chains and/or coagulation/coalescence of already formed particles. This process depends essentially on the concentration of available hydrophilic chains and hence on the target molar mass of the hydrophobic block (at constant concentration of hydrophobic monomer). Moreover, the final particle morphology, which depends on the pH of the continuous water phase as shown above, is also dictated by the volume occupied by the stabilizing segments at the particle surface in strongly segregated systems. At low pH where the P(MAA-*co*-PEOMA) backbone is not charged, the segregation strength between the blocks is probably not large enough and the spherical morphology remains the most favorable one, with possible burial of some of the hydrophilic segments into the polymer core. This was illustrated by the presence of holes in the biggest particles (especially in series B, Figure 2), indicative of the presence of segregated hydrophilic segments swollen by water, which evaporates upon drying. Such behavior was previously observed in RAFT-mediated miniemulsion polymerization of styrene in the presence of a PEO-based macroRAFT agent.[53]

CONCLUSIONS

The RAFT emulsion polymerization of styrene was carried out in one-pot, via a two-step process using two P(MAA-*co*-PEOMA) macroRAFT agents with different compositions. The latter were prepared *in situ*, directly in aqueous solution at acidic pH. In all cases, their synthesis was fast and efficient, leading to very high conversions and very good control over the polymer features. It was moreover particularly reproducible, which is an important outcome for the robustness of the method. Besides being of high interest in terms of reaction time and respect of environmental constraints, the emulsion polymerizations led to kinetic results that were rich in information concerning the particle formation and growth mechanism. Indeed, the very good control over reinitiation and chain growth as well as the formation of particles with very narrow particle size distribution allowed the system to be studied accurately. The nucleation occurred via self-assembly of *in situ* formed amphiphilic block copolymers. The particle size and stabilization were controlled by the surface coverage by the hydrophilic segment rather than the initial aggregation number. In other words, reorganization of the particles during their growth appeared to be a key step in the mechanism.

ASSOCIATED CONTENT

Ⓢ Supporting Information. Kinetic study of the aqueous copolymerization of MAA and PEOMA; description of the "two-pot" emulsion polymerizations. This material is available free of charge via the Internet at http://pubs.acs.org.

ACKNOWLEDGMENT

The authors thank the University of Lyon and the French Ministry of Research for WZ's PhD grant. B.C. is grateful to the IUF (Institut Universitaire de France) for her nomination as senior member. The CTμ (Centre Technologique des Microstructures) is acknowledged for the TEM analyses.

REFERENCES

(1) Matyjaszewski, K.; Davis, T. P. In *Handbook of Radical Polymerization*; Wiley-Interscience: Hoboken, NJ, 2002.

(2) Braunecker, W. A.; Matyjaszewski, K. *Prog. Polym. Sci.* **2007**, *32*, 93–146.

(3) Barner-Kowollik, C., Ed. *Handbook of RAFT Polymerization*; Wiley-VCH: Weinheim, 2008.

(4) Matyjaszewski, K., Gnanou, Y., Leibler, L., Eds. *Macromolecular Engineering: Precise Synthesis, Materials Properties, Applications*; Wiley-VCH: Weinheim, 2007; Vol. 1.

(5) Jenkins, A. D.; Jones, R. G.; Moad, G. *Pure Appl. Chem.* **2010**, *82*, 483–491.

(6) Gilbert, R. G. *Emulsion Polymerization. A Mechanistic Approach*; Academic Press: New York, 1995.

(7) Qiu, J.; Charleux, B.; Matyjaszewski, K. *Prog. Polym. Sci.* **2001**, *26*, 2083–2134.

(8) Monteiro, M.; Charleux, B. In *Chemistry and Technology of Emulsion Polymerisation*; van Herk, A., Ed.; Blackwell Publishing Ltd.: Oxford, 2005; Chapter 5, pp 111−139.

(9) Save, M.; Guillaneuf, Y.; Gilbert, R. G. *Aust. J. Chem.* **2006**, *59*, 693–711.

(10) McLeary, J. B.; Klumperman, B. *Soft Matter* **2006**, *2*, 45–53.

(11) Cunningham, M. F. *Prog. Polym. Sci.* **2008**, *33*, 365–398.

(12) Zetterlund, P. B.; Kagawa, Y.; Okubo, M. *Chem. Rev.* **2008**, *108*, 3747–3794.

(13) Charleux, B.; Nicolas, J. *Polymer* **2007**, *48*, 5813–5833.

(14) Charleux, B.; D'Agosto, F.; Delaittre, G. *Adv. Polym. Sci.* **2010**, *233*, 125–183.

(15) Delaittre, G.; Nicolas, J.; Lefay, C.; Save, M.; Charleux, B. *Chem. Commun.* **2005**, 615–616.

(16) Delaittre, G.; Nicolas, J.; Lefay, C.; Save, M.; Charleux, B. *Soft Matter* **2006**, *2*, 223–231.

(17) Delaittre, G.; Save, M.; Charleux, B. *Macromol. Rapid Commun.* **2007**, *28*, 1528–1533.

(18) Delaittre, G.; Charleux, B. *Macromolecules* **2008**, *41*, 2361–2367.

(19) Dire, C.; Magnet, S.; Couvreur, L.; Charleux, B. *Macromolecules* **2009**, *42*, 95–103.

(20) Brusseau, S.; Belleney, J.; Magnet, S.; Couvreur, L.; Charleux, B. *Polym. Chem.* **2010**, *1*, 720–729.

(21) Okubo, M.; Sugihara, Y.; Kitayama, Y.; Kagawa, Y.; Minami, H. *Macromolecules* **2009**, *42*, 1979–1984.

(22) Kitayama, Y.; Moribe, H.; Minami, H.; Okubo, M. *Polymer* **2011**, *52*, 2729–2734.

(23) Ferguson, C. J.; Hughes, R. J.; Pham, B. T. T.; Hawkett, B. S.; Gilbert, R. G.; Serelis, A. K.; Such, C. H. *Macromolecules* **2002**, *25*, 9243–9245.

(24) Ferguson, C. J.; Hughes, R. J.; Nguyen, D.; Pham, B. T. T.; Gilbert, R. G.; Serelis, A. K.; Such, C. H.; Hawkett, B. S. *Macromolecules* **2005**, *38*, 2191–2204.

(25) Manguian, M.; Save, M.; Charleux, B. *Macromol. Rapid Commun.* **2006**, *27*, 399–404.

(26) Sprong, E.; Leswin, J. S. K.; Lamb, D. J.; Ferguson, C. J.; Hawkett, B. S.; Pham, B. T. T.; Nguyen, D.; Such, C. H.; Serelis, A. K.; Gilbert, R. G. *Macromol. Symp.* **2006**, *231*, 84–93.

(27) Ganeva, D. E.; Sprong, E.; de Bruyn, H.; Warr, G. G.; Such, C. H.; Hawkett, B. S. *Macromolecules* **2007**, *40*, 6181–6189.

(28) Božović-Vukić, J.; Mañon, H. T.; Meuldijk, J.; Koning, C.; Klumperman, B. *Macromolecules* **2007**, *40*, 7132–7139.

(29) Rieger, J.; Stoffelbach, F.; Bui, C.; Alaimo, D.; Jérôme, C.; Charleux, B. *Macromolecules* **2008**, *41*, 4065–4068.

(30) Urbani, C. N.; Monteiro, M. J. *Macromolecules* **2009**, *42*, 3884–3886.

(31) Rieger, J.; Osterwinter, G.; Bui, C.; Stoffelbach, F.; Charleux, B. *Macromolecules* **2009**, *42*, 5518–5525.

(32) Wang, X.; Luo, Y.; Li, B.; Zhu, S. *Macromolecules* **2009**, *42*, 6414–6421.

(33) Luo, Y.; Wang, X.; Li, B.-G.; Zhu, S. *Macromolecules* **2011**, *44*, 221–229.

(34) Wei, R. Z.; Luo, Y. W.; Xu, P. H. *J. Polym. Sci., Part A: Polym. Chem.* **2011**, *49*, 2980–2989.

(35) Rieger, J.; Zhang, W.; Stoffelbach, F.; Charleux, B. *Macromolecules* **2010**, *43*, 6302–6310.

(36) Yeole, N.; Hundiwale, D.; Jana, T. *J. Colloid Interface Sci.* **2011**, *354*, 506–510.

(37) Delaittre, G.; Dire, C.; Rieger, J.; Putaux, J.-L.; Charleux, B. *Chem. Commun.* **2009**, 2887–2889.

(38) Boissé, S.; Rieger, J.; Belal, K.; Di-Cicco, A.; Beaunier, P.; Li, M.-H.; Charleux, B. *Chem. Commun.* **2010**, *46*, 1950–1952.

(39) Zhang, X.; Boissé, S.; Zhang, W.; Beaunier, P.; D'Agosto, F.; Rieger, J.; Charleux, B. *Macromolecules* **2011**, *44*, 4149–4158.

(40) Boissé, S.; Rieger, J.; Pembouong, G.; Beaunier, P.; Charleux, B. *J. Polym. Sci., Part A: Polym. Chem.* **2011**, *49*, 3346–3354.

(41) Boursier, T.; Chaduc, I.; Rieger, J.; D'Agosto, F.; Lansalot, M.; Charleux, B. *Polym. Chem.* **2011**, *2*, 355–362.

(42) Chaduc, I.; Zhang, W.; Rieger, J.; Lansalot, M.; D'Agosto, F.; Charleux, B. *Macromol. Rapid Commun.* **2011**, *32*, 1270–1276.

(43) Brusseau, S.; D'Agosto, F.; Magnet, S.; Couvreur, L.; Chamignon, C.; Charleux, B. *Macromolecules* **2011**, *44*, 5590–5598.

(44) Xu, X.; Smith, A. E.; Kirkland, S. E.; McCormick, C. L. *Macromolecules* **2008**, *41*, 8429–8435.

(45) Couvreur, L.; Lefay, C.; Belleney, J.; Charleux, B.; Guerret, O.; Magnet, S. *Macromolecules* **2003**, *36*, 8260–8267.

(46) Rinaldi, D.; Hamaide, T.; Graillat, C.; D'Agosto, F.; Spitz, R.; Georges, S.; Mosquet, M.; Maitrasse, P. *J. Polym. Sci., Part A: Polym. Chem.* **2009**, *47*, 3045–3055.

(47) Tan, Y. Y.; Challa, G. *Makromol. Chem., Macromol. Symp.* **1987**, *10/11*, 215–233.

(48) Bekturov, E.; Bimendina, L. *Adv. Polym. Sci.* **1981**, *41*, 99–147.

(49) (a) Astafieva, I.; Zhong, X. F.; Eisenberg, A. *Macromolecules* **1993**, *26*, 7339–7352. (b) Khougaz, K.; Astafieva, I.; Eisenberg, A. *Macromolecules* **1995**, *28*, 7135–7147.

(50) Burguière, C.; Chassenieux, C.; Charleux, B. *Polymer* **2003**, *44*, 509–518.

(51) Luo, Y.; Wang, R.; Yang, L.; Yu, B.; Li, B.; Zhu, S. *Macromolecules* **2006**, *39*, 1328–1337.

(52) Chiefari, J.; Mayadunne, R. T. A.; Moad, C. L.; Moad, G.; Rizzardo, E.; Postma, A.; Skidmore, M. A.; Thang, S. H. *Macromolecules* **2003**, *36*, 2273–2283.

(53) Martins dos Santos, A.; Le Bris, T.; Graillat, C.; D'Agosto, F.; Lansalot, M. *Macromolecules* **2009**, *42*, 946–956.

(54) Buback, M.; Gilbert, R. G.; Hutchinson, R. A.; Klumpermann, B.; Kuchta, F.-D.; Manders, B. G.; O'Driscoll, K. F.; Russell, G. T.; Schweer, J. *Macromol. Chem. Phys.* **1995**, *196*, 3267–3280.